Bioorganic Chemistry 165 (2025) 108931

Contents lists available at ScienceDirect

Bioorganic Chemistry

journal homepage: www.elsevier.com/locate/bioorg

Structural hybridization of alepterolic acid with piperazine-benzamide motifs yields potent anticancer agents☆

Xin Wang [a,b,1], Lian Ma [a,1], Yanchun Sun [b], Zixuan Tong [b], Binbin Zhang [a], Yating Jia [a], Xiling Dai [a], Jianguo Cao [a,*], Guozheng Huang [b,*]

[a] College of Life Sciences, Shanghai Normal University, Shanghai, PR China
[b] School of Chemistry and Chemical Engineering, Anhui University of Technology, Ma'anshan, PR China

ARTICLE INFO

Keywords:
Alepterolic acid
Structural modification
Piperazine
Breast cancer
Hybrid

ABSTRACT

Among the most pervasive malignancies affecting females worldwide, breast cancer is responsible for approximately 2.2 million new diagnoses and over 660,000 fatalities reported annually. Natural products represent an invaluable resource for the identification and development of potential innovative anti-cancer pharmaceuticals. In our present study, two series of derivatives were designed for synthesis by merging benzamide and piperazine with alepterolic acid. According to our observations, compounds **11s** and **13r** were cytotoxically more active against the MCF-7 cell line, showing IC_{50} values of 4.93 ± 0.84 μM and 2.95 ± 0.52 μM, respectively. Further investigations revealed that under the treatment with **11s** and **13r**, morphology of MCF-7 cells was changed and their growth was inhibited both dose- and time-dependently. Additional Western blotting demonstrated a marked increase in the levels of cleaved caspases−3, −8, −9, cleaved poly (ADP ribose) polymerase (PARP) alongside Bax/Bcl-2 ratio in the **11s**-treated MCF-7 cells. Similarly, treatment with **13r** significantly upregulated the cellular cleaved caspases−3, −8, and PARP levels. Mechanistically, Western blotting revealed that **11s** triggered both the intrinsic (via cleaved caspase−9/Bax upregulation) and extrinsic (via cleaved caspase−8 activation) apoptosis in MCF-7 cells, whereas **13r** solely activated the extrinsic pathway. Conclusively, our findings demonstrated that the incorporation of benzamide and piperazine to alepterolic acid represents a promising approach for the discovery of new drug candidates.

1. Introduction

The past half century witnessed a rapid increase in cancer-related morbidity and mortality. The International Agency for Research on Cancer statistics position breast cancer as one of the most pervasive malignancies affecting women globally. The World Health Organization predicts that by 2025, the global death toll from cancer will reach 13 million [1]. Chemotherapy, radiation therapy, and immunotherapy are the current mainstream approaches to cancer treatment. During chemotherapy, patients receive anti-cancer drugs, which not only kill cancer cells but also damage healthy tissues, leading to drug resistance and various adverse reactions. Hence, developing innovative and safe anticancer therapeutics is critically needed [2,3].

Natural products constitute a significant reservoir for the exploration and development of novel antineoplastic alternatives [4,5]. To date, numerous natural products have been recognized as medicinal agents with significant biological activities, including artemisinin (antimalarial drug) [6], paclitaxel (anticancer drug) [7], morphine (analgesic drug) [8] and daptomycin (antibacterial drug) [9,10]. A category of natural products called diterpenoids are typified by the presence of four isoprene units. In recent years, multiple diterpenoid compounds have been extensively investigated and developed as potential anticancer agents [11,12]. Tanshinone IIA (**1**, Fig. 1), an abietane-type diterpenoid isolated from *Salvia miltiorrhiza*, features a characteristic *ortho*-quinone moiety fused with a tetrahydronaphthalene ring [13]. It possesses antineoplastic properties, which manifest in the suppression of gastric carcinoma cell proliferation by triggering the p53-dependent ferroptosis [14,15]. Yunnancoronarin A (**2**, Fig. 1), a rearranged labdane-type diterpenoid extracted from the rhizomes of *Hedychium forrestii*, demonstrates cytotoxicity against K562 myelogenous leukemia cells, with an

☆ This article is part of a Special issue entitled: 'Targeted cancer therapy' published in Bioorganic Chemistry.

* Corresponding authors.
E-mail addresses: cao101@shnu.edu.cn (J. Cao), guozheng.huang@ahut.edu.cn (G. Huang).

[1] These authors contribute equally.

https://doi.org/10.1016/j.bioorg.2025.108931
Received 19 June 2025; Received in revised form 16 August 2025; Accepted 28 August 2025
Available online 30 August 2025

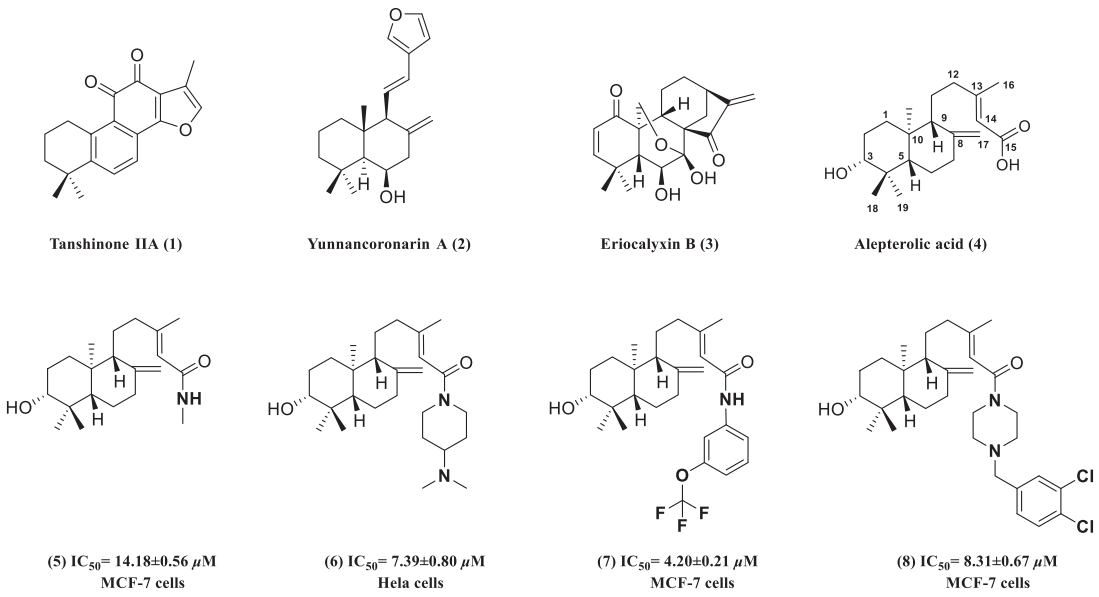

Fig. 1. Chemical structures of alepterolic acid along with related natural compounds.

IC_{50} of 2.20 μM [16,17]. Eriocalyxin B (**3**, Fig. 1), an *ent*-kaurane diterpenoid extract of *Isodon eriocalyx*, exhibits potent anti-tumor activity. Eriocalyxin B is expected to inhibit the progression of breast cancer by regulating mast cells [18].

Alepterolic acid (**4**, Fig. 1) refers to an *ent*-labdane-type diterpene isolate of *Aleuritopteris argentea* [19,20]. Labdane-type diterpenoids and their derivatives have been reported to exhibit remarkable potential for applications in anti-inflammatory, anti-antioxidant, and anti-cancer treatment [21–26]. Nevertheless, the biological properties of alepterolic acid and its derivatives remain poorly characterized. Previously, we

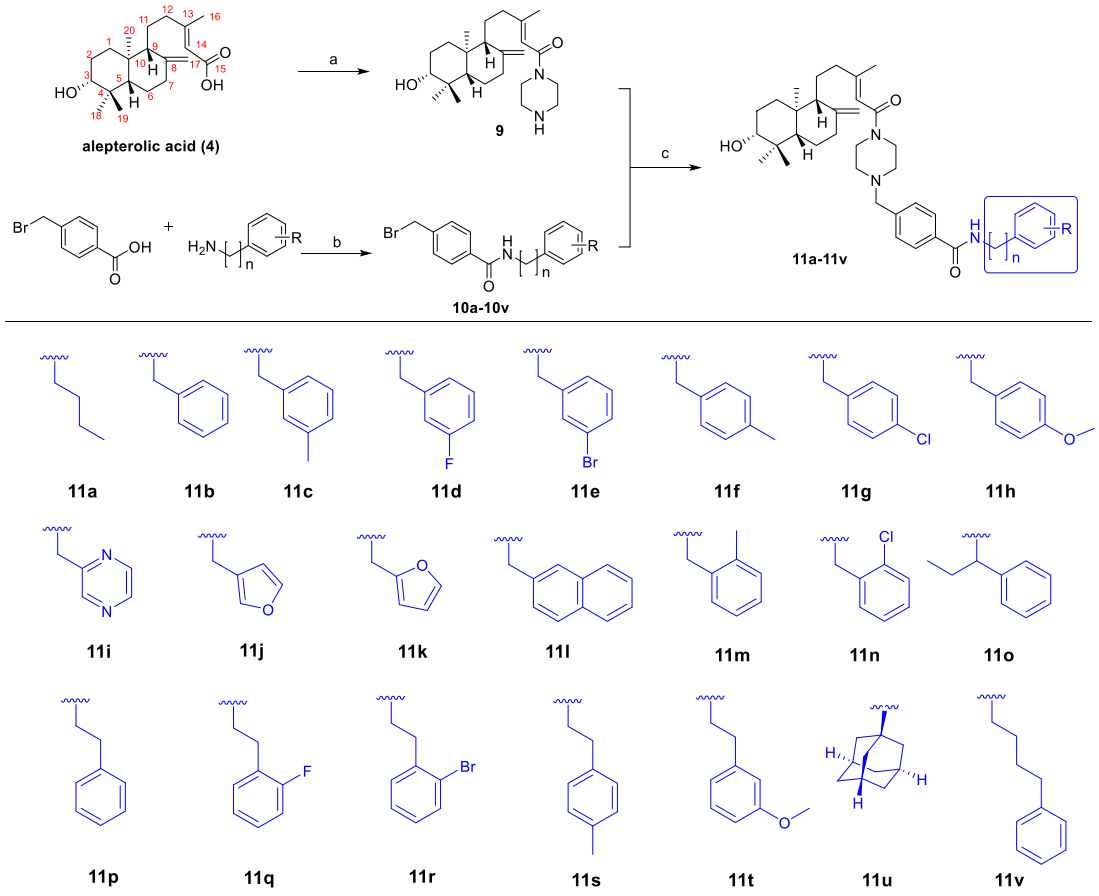

Scheme 1. Synthesis of benzyl piperazinyl derivatives of alepterolic acid (**11a-11v**). Reaction settings: (a) HATU, *N,N*-diisopropylethylamine, piperazine, CH_2Cl_2, r. t., 3 h; (b) Oxalyl chloride, CH_2Cl_2, cat. DMF, r.t., 2 h; (c) DIPEA, CH_3CN, r.t., 20 h.

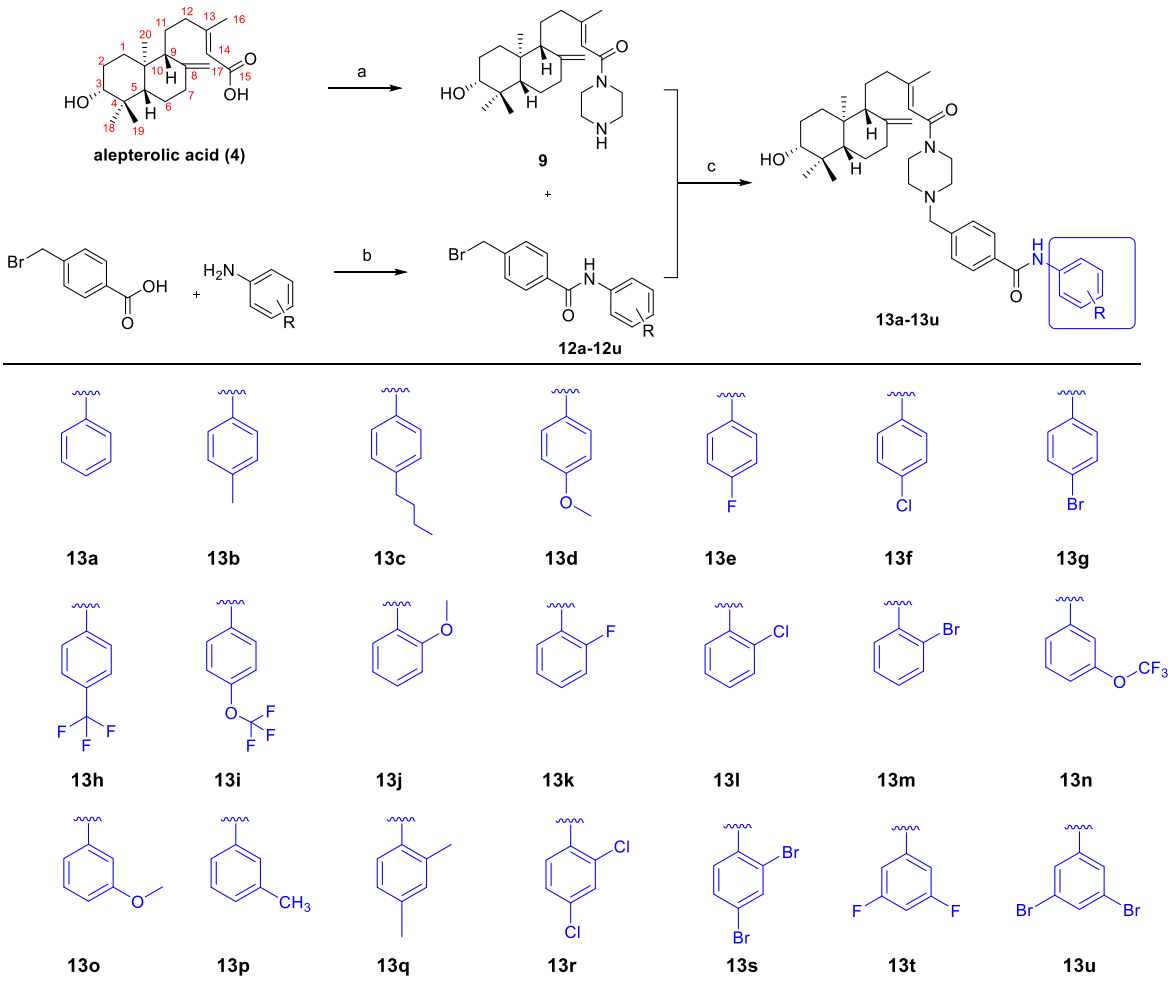

Scheme 2. Synthesis of benzyl piperazinyl derivatives of alepterolic acid (**13a-13u**). Reaction settings: (a) HATU, *N,N*-diisopropylethylamine, piperazine, CH_2Cl_2, r. t., 3 h; (b) Oxalyl chloride, CH_2Cl_2, cat. DMF, r.t., 2 h; DIPEA, CH_3CN, r.t., 20 h.

functionalized the C-15 carboxyl group of alepterolic acid by amidation reaction. Compared to alepterolic acid, *N*-methyl alepterolamide (**5**, Fig. 1) exhibited a higher MCF-7 cell cytotoxicity, with IC_{50} was 14.18 ± 0.56 μM. Compound **6** (Fig. 1), with a *N,N*-dimethyl-4-piperidinamine moiety, demonstrated an IC_{50} of 7.39 ± 0.80 μM toward human cervical carcinoma HeLa cells. This compound stimulates the mitochondrial cytochrome *c* secretion, leading to the caspases−3, −9 cleavage and activation, as well as the PARP cleavage. Consequently, it results in the cessation of HeLa cell DNA repair and induces intrinsic apoptosis [27]. Additionally, a range of innovative aniline derivatives of alepterolic acid have been synthesized, among which compound **7** (Fig. 1) displays the strongest potency for MCF-7 cell suppression, recording an IC_{50} of 4.20 ± 0.21 μM. This derivative exerts a significant anti-proliferative action on MCF-7 cells and reverses EMT to inhibit cell migration. It also regulates the Akt/$p70^{S6K}$ signaling pathway to induce apoptosis [28]. More recently, we introduced benzylpiperazine moiety at the C-15 carboxyl position of alepterolic acid, yielding a series of derivatives. Among them, compound **8** (Fig. 1) displays the strongest potency for suppressing MCF-7 cells, with an IC_{50} value of 8.31 ± 0.67 μM. It can lyse and activate caspases−3 and -9, leading to the PARP cleavage and loss of DNA repair function in MCF-7 cells, ultimately inducing intrinsic apoptosis [29].

Piperazine functions as a privilege structure in a variety of natural and synthetic compounds, exhibiting a broad spectrum of anticancer activities [30–33]. Piperazinyl derivatives of natural products possess good biological activity against breast cancer cells [34]. In light of these findings, the present study introduced piperazine to alepterolic acid, with the attachment of a benzamide structure, for synthesizing two series of new compounds and subsequently evaluated their anticancer potency.

2. Results and discussion

2.1. Chemistry

Based on our previous reports, intermediate piperazinyl alepterolic amide (**9**) can be easily synthesized from alepterolic acid (**4**) by using condensation agents such as 2-(7-azabenzotriazol-1-yl)-*N,N,N′,N′*-tetramethyluronium hexafluorophosphate (HATU). Subsequently, a reduction amination or alkylation reaction was employed to produce phenylamino-benzyl piperazine derivatives (**11** and **13**). Compared to reduction amination, alkylation requires fewer reagents and simpler procedures. As illustrated in Schemes 1 and 2, 4-bromomethyl benzoic acid was converted into the corresponding acyl chloride by oxalyl chloride, where *N,N*-dimethylformamide (DMF) was used as the catalyst. This acyl chloride then underwent amidation with various anilines or alkylamines to form intermediate (**10a-10v** and **12a-12u**). The final step involved benzylation of compound (**9**) with various benzyl bromide (**10a-10v** and **12a-12u**) in the presence of *N,N*-diisopropylethylamine (DIPEA) to afford compounds **11a-11v** and **13a-13u**. We maintained diversity in the amine substrates, including alkylamines (e.g. **11a**, **11u**), electron-donating groups (e.g. **11f**, **11h**, **13b**, **13d**), electron-withdrawing groups (e.g. **13h**), sterically hindered groups (e.g. **11o**),

Table 1
Cytotoxic screening of phenylamino-benzyl piperazine derivatives of alepterolic acid against three cancer cell types and a normal human liver cell line.

Compounds	Cell lines (IC_{50}/μM*)			
	MDA-MB-231	A549	MCF-7	HL-7702
11a	45.29 ± 9.73	12.99 ± 0.96	18.31 ± 1.44	15.25 ± 2.15
11b	25.05 ± 2.27	11.02 ± 1.62	18.77 ± 4.74	22.62 ± 2.21
11c	30.7 ± 2.06	11.06 ± 0.96	19.94 ± 1.30	18.1 ± 2.04
11d	30.54 ± 4.02	13.51 ± 2.47	18.28 ± 1.68	13.8 ± 1.90
11e	46.42 ± 2.10	13.30 ± 2.01	21.63 ± 3.33	14.68 ± 2.99
11f	25.53 ± 1.53	6.82 ± 0.73	17.41 ± 2.71	3.86 ± 1.21
11g	16.38 ± 1.92	5.77 ± 1.00	9.00 ± 2.70	18.29 ± 2.68
11h	27.66 ± 1.77	12.81 ± 2.29	19.39 ± 2.96	25.41 ± 2.00
11i	>100	>100	65.91 ± 17.90	>100
11j	29.76 ± 1.53	13.68 ± 1.58	17.68 ± 1.51	16.12 ± 4.12
11k	25.47 ± 3.52	12.19 ± 2.83	23.64 ± 4.01	17.88 ± 1.94
11l	73.25 ± 14.64	10.49 ± 2.17	7.71 ± 2.30	5.85 ± 1.34
11m	22.51 ± 1.72	7.99 ± 1.60	11.09 ± 3.94	6.57 ± 1.78
11n	60.00 ± 7.38	11.25 ± 1.96	13.66 ± 1.85	5.41 ± 1.16
11o	40.66 ± 3.84	9.64 ± 2.01	11.02 ± 3.31	5.85 ± 1.74
11p	30.86 ± 0.80	7.19 ± 0.88	8.13 ± 0.89	16.28 ± 2.13
11q	29.69 ± 1.26	7.63 ± 0.70	14.62 ± 1.48	11.04 ± 1.18
11r	>100	13.03 ± 2.74	14.37 ± 2.32	12.34 ± 1.22
11s	13.35 ± 0.98	3.56 ± 0.47	4.93 ± 0.84	7.76 ± 0.76
11t	63.85 ± 5.80	22.55 ± 2.47	23.23 ± 2.68	39.6 ± 4.67
11u	54.61 ± 3.06	30.51 ± 7.73	21.34 ± 2.73	3.35 ± 0.72
11v	69.09 ± 4.64	11.53 ± 1.89	17.88 ± 3.29	42.86 ± 3.98
13a	49.37 ± 2.20	7.73 ± 1.46	6.48 ± 1.14	26.04 ± 2.44
13b	46.57 ± 3.73	9.73 ± 2.49	8.81 ± 1.13	20.26 ± 1.47
13c	>100	29.26 ± 1.67	17.00 ± 0.86	78.79 ± 22.70
13d	76.5 ± 8.34	15.63 ± 3.21	17.61 ± 2.39	29.44 ± 1.94
13e	69.37 ± 9.11	8.20 ± 1.91	10.34 ± 1.94	17.89 ± 1.98
13f	>100	10.95 ± 3.39	14.03 ± 1.93	12.21 ± 3.28
13g	>100	6.67 ± 2.45	14.02 ± 1.78	7.19 ± 2.33
13h	>100	9.64 ± 2.53	5.37 ± 0.34	6.11 ± 1.48
13i	>100	9.87 ± 1.60	15.9 ± 11.57	3.71 ± 0.90
13j	24.72 ± 0.80	13.11 ± 1.74	13.92 ± 2.04	18.27 ± 1.98
13k	25.43 ± 2.11	4.06 ± 1.24	6.60 ± 0.97	10.06 ± 2.13
13l	35.19 ± 2.04	8.43 ± 1.42	14.13 ± 1.07	18.58 ± 2.23
13m	27.35 ± 0.86	6.34 ± 1.05	5.82 ± 1.25	13.52 ± 3.40
13n	>100	7.38 ± 2.54	10.66 ± 7.06	4.065 ± 2.53
13o	>100	69.84 ± 17.07	>100	>100
13p	>100	13.66 ± 2.69	13.05 ± 1.98	19.77 ± 4.11
13q	>100	24.49 ± 3.61	52.92 ± 9.97	>100
13r	47.33 ± 7.77	3.51 ± 0.93	2.95 ± 0.52	4.68 ± 0.54
13s	>100	6.36 ± 2.52	5.18 ± 1.24	9.94 ± 3.14
13t	>100	9.08 ± 2.73	5.92 ± 0.90	12.67 ± 1.33
13u	>100	38.81 ± 11.30	>100	39.19 ± 7.03
Camptothecin	1.44 ± 0.69	0.42 ± 0.09	0.22 ± 0.09	0.12 ± 0.03

* After 72 h of treatment with compounds, the cells were examined for viability by the MTT assay. Quantitative data are reported as means ± SDs from a minimum of triplicate independent experiments. Cell viability rate (%) = (A_{sample}-A_{blank})/($A_{control}$-A_{blank})*100.

and some heterocycles (e.g. **11i**, **11j**, **11k**). The synthesized compounds were subjected to HRMS, ^{1}H NMR, and ^{13}C NMR characterization. For instance, in the ^{1}H NMR spectrum of compound **11h**, the signals of methylene of benzyl group appeared at δ 3.54 ppm as doublet; the signals of the aromatic protons descended from 4-bromomethyl benzoic acid appeared at the range of δ 7.74–7.36 ppm as doublet peaks; the signals of aromatic protons descended from aromatic amines appeared as doublet peak at the ranges of δ 7.28–6.81 ppm; the signal of methylene of benzyl group was observed at δ 62.43 ppm in the ^{13}C NMR spectrum; the signals of four carbon atoms in piperazine structure were noted at δ 55.18, 53.01, 46.28 and 41.17, respectively. A consistency was found between the analytical and structural data.

2.2. Cytotoxicity evaluation of synthesized compounds

Cancer represents a significant global health challenge, which has emerged as a leading cause of mortality. Accordingly, the design and development of innovative anticancer therapeutics is among the most pressing areas of research [35]. In recent years, breast cancer has emerged as one of the globally most pervasive malignancies among females, with persistently increasing incidence and mortality rates. Prior research has demonstrated that certain derivatives of alepterolic acid exhibit potent inhibitory activity against breast cancer cells. In the present study, MTT assay was utilized to determine the *in vitro* semi-inhibitory concentration (IC_{50}) values of target compounds toward cancerous MDA-MB-231, MCF-7, A549 versus healthy liver HL-7702 cells, where camptothecin served as the positive control. As illustrated in Table 1, a significant cytotoxicity variation was observed among the compounds, which was contingent upon the substituent group associated with the phenylamino-benzyl piperazine moiety. The aniline-substituted amide compounds demonstrated superior activity to those aliphatic amines-substituted. Good inhibitory activity was found with the aniline-substituted derivative (**13a**), with IC_{50} values of 6.48 ± 1.14 μM and 7.73 ± 1.46 μM in MCF-7 and A549 cells, respectively.

Among the aliphatic amines-substituted derivatives (**11a-11v** series), compound **11d** exhibited superior toxicity to compound **11e**, indicating that the F substituent is preferable to Br. This is further substantiated by the comparison between compounds **11q** and **11r**. Additionally, compound **11g** displayed higher toxicity than compound **11f**, while compound **11h** showed the lowest toxicity, suggesting that the Cl substituent is more favorable than -CH_3, and -OCH_3 is the least effective. The substitution of phenethylamine (**11p)** yielded better activity than that of benzylamine (**11b**), recording respective IC_{50} of 7.19 ± 0.88 μM and 8.13 ± 0.89 μM in A549 and MCF-7 cells. Furthermore, the introduction of halogen elements based on benzylamine and phenylethylamine resulted in an activity decline. The α-naphthylamine derivative (**11*l***) also demonstrated efficacy against A549 and MCF-7 cells, with respective IC_{50} being 10.49 ± 2.17 μM and 7.71 ± 2.3 μM. This suggests that the bulky group might be tolerated.

Within the **13a-13u** series derivatives, compound **13h** was the best *para*-substituent (**13b-13i**) derivative, whose anti-MCF-7 activity was higher than that of **13a**, recording an IC_{50} of 5.37 ± 3.34 μM. This implies that the activity can be enhanced by introducing trifluoromethyl at the *para*-position, whereas the introduction of methoxy groups (**13d**, **13j**, and **13o**) was ineffective. The activity of compound **13k** with a *meta*-fluorine group was better to that of compound **13a** and surpassed that of compound **13e** with a *para*-fluorine group for MCF-7 cells. Among the *ortho*-substituted derivatives (**13j-13m**), compound **13m** recorded the best IC_{50} value of 5.82 ± 1.25 μM. In MCF-7 cells, the compound **13l** containing an *ortho*- chlorine group was somewhat as active as the compound **13f** containing a *para*-chlorine group. With two chlorine atoms were introduced at the *ortho*-position and *para*-position, we identified compound **13r** as the strongest compound of all the synthesized derivatives in this study, whose IC_{50} was 2.95 ± 0.52 μM for MCF-7 cells and 4.68 ± 0.54 for normal liver HL-7702 cells.

Camptothecin is a potent anticancer drug extracted from the *Camptotheca acuminata* Decne. It works by inhibiting topoisomerase I, thereby disrupting DNA replication in cancer cells [36,37]. Compared to the positive control drug camptothecin, compounds **11s** and **13r** exhibited weaker cytotoxicity. However, they demonstrated higher selectivity, with compound **11s** showing stronger toxicity toward MCF-7 cells than MDA-MB-231 cells. Additionally, both compounds exhibited relatively low toxicity against normal hepatocytes (HL-7702), suggesting potentially reduced side effects in humans. The aforementioned findings indicate that **11s** (IC_{50} = 4.93 ± 0.84 μM) and **13r** (IC_{50} = 2.95 ± 0.52 μM) exhibit comparatively higher toxicity against the breast cancer MCF-7 cells. Subsequently, we focused on further biological evaluation to elucidate the underlying mechanisms of action of these two compounds in MCF-7 cells.

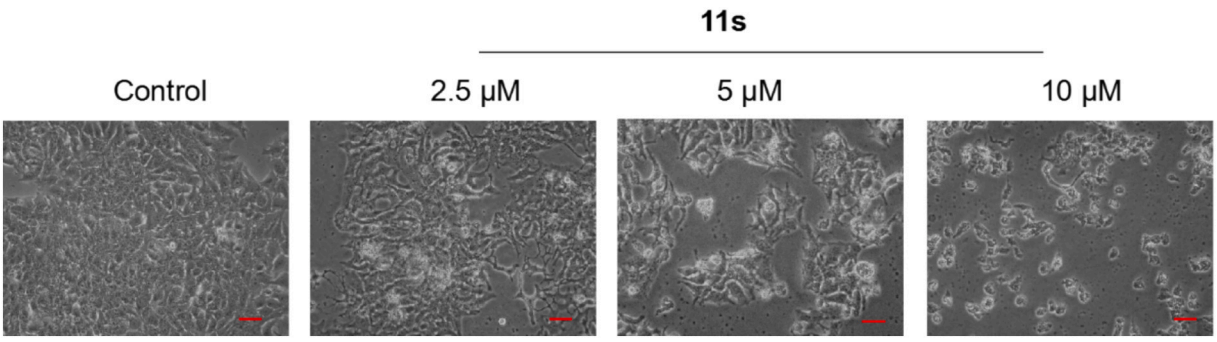

Fig. 3. Cellular morphological alterations in response to **11s**. Non-treated MCF-7 cells and those subjected to a 24-h gradient compound **11s** (0, 2.5, 5, 10 μM) treatment. (Scale bar: 50 μm)

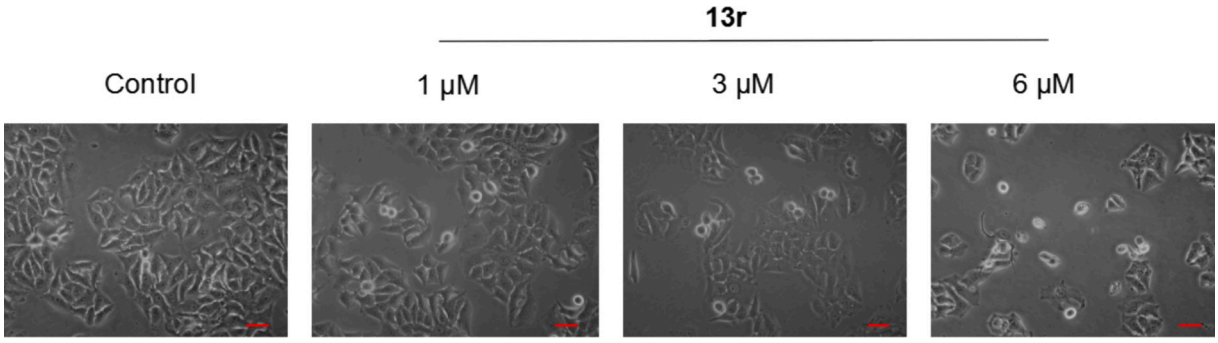

Fig. 4. Cellular morphological alterations in response to **13r**. Non-treated MCF-7 cells and those subjected to a 24-h gradient compound **13r** (0, 1, 3 and 6 μM) treatment. (Scale bar: 50 μm).

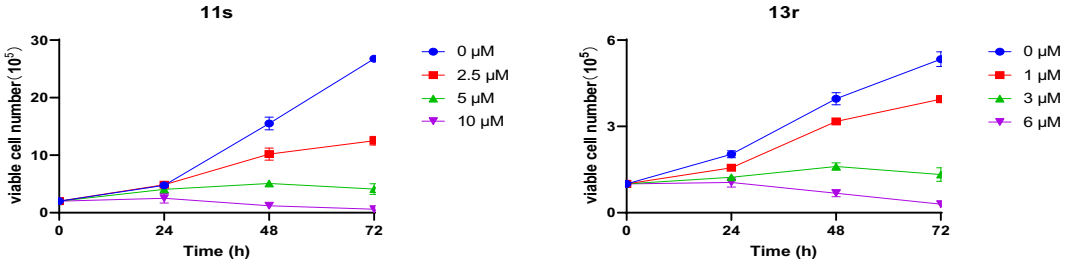

Fig. 5. Compounds **11s** and **13r** inhibited the MCF-7 cell growth. Growth curves after 24, 48 and 72 h of **11s** and **13r** treatment.

*2.3. Compounds **11s** and **13r** inhibited the growth of MCF-7 cells*

To investigate the cellular impacts of **11s** and **13r**, we exposed MCF-7 cells to diverse concentrations of **11s** and **13r**. At 24 h post-treatment, cellular morphological alterations were observed through optical microscopy, and the outcomes were presented in Figs. 3 and 4. The morphology of cells serves as a critical structural foundation for their biological functions [38,39]. With the rise in the concentration of compounds **11s** and **13r**, the quantity of MCF-7 cells gradually declined. At the highest doses (**11s**, 10 μM; **13r**, 6 μM), microscopic analysis revealed characteristic cellular responses including contraction, dispersion, and subsequent detachment from the culture substrate. Furthermore, the number of floating cells gradually increased, presenting a transparent and shiny state as the compound concentration rose. As implied by the above results, **11s** and **13r** might inhibit the growth of MCF-7 cells and induce their demise dose-dependently. Next, we conducted a further investigation into the effects of these two compounds on the MCF-7 cell growth through Trypan blue staining, one of the most classical methods for identifying the cell survival rate in culture, which enables a facile and rapid distinction between living and dead cells [40]. We found that normal cells remained uncolored, while dead and dying cells were stained blue by Trypan blue. Further, the growth curves of cells following drug treatment were fitted by cell counting and software analysis. As depicted in Fig. 5, a significant reduction in cell viability was observed upon exposure to compounds **11s** and **13r**. These results indicated a concentration- and time-dependent inhibition of MCF-7 cell growth by **11s** and **13r**.

*2.4. Compounds **11s** and **13r** suppressed the formation of MCF-7 cell colonies*

To further prove that compounds **11s** and **13r** can inhibit the growth of MCF-7 cells, we further investigated their effects on the cellular colony-forming capacity through plate clone formation experiments. According to Fig. 6, the colony formation gradually weakened as the drug concentration rose, which was even completely inhibited at high doses (**11s**, 10 μM; **13r**, 6 μM), showing significant differences from the controls (*** $p < 0.001$). Suggestively, **11s** and **13r** can exert prolonged dose-dependent inhibitory effects on the formation of MCF-7 cell colonies.

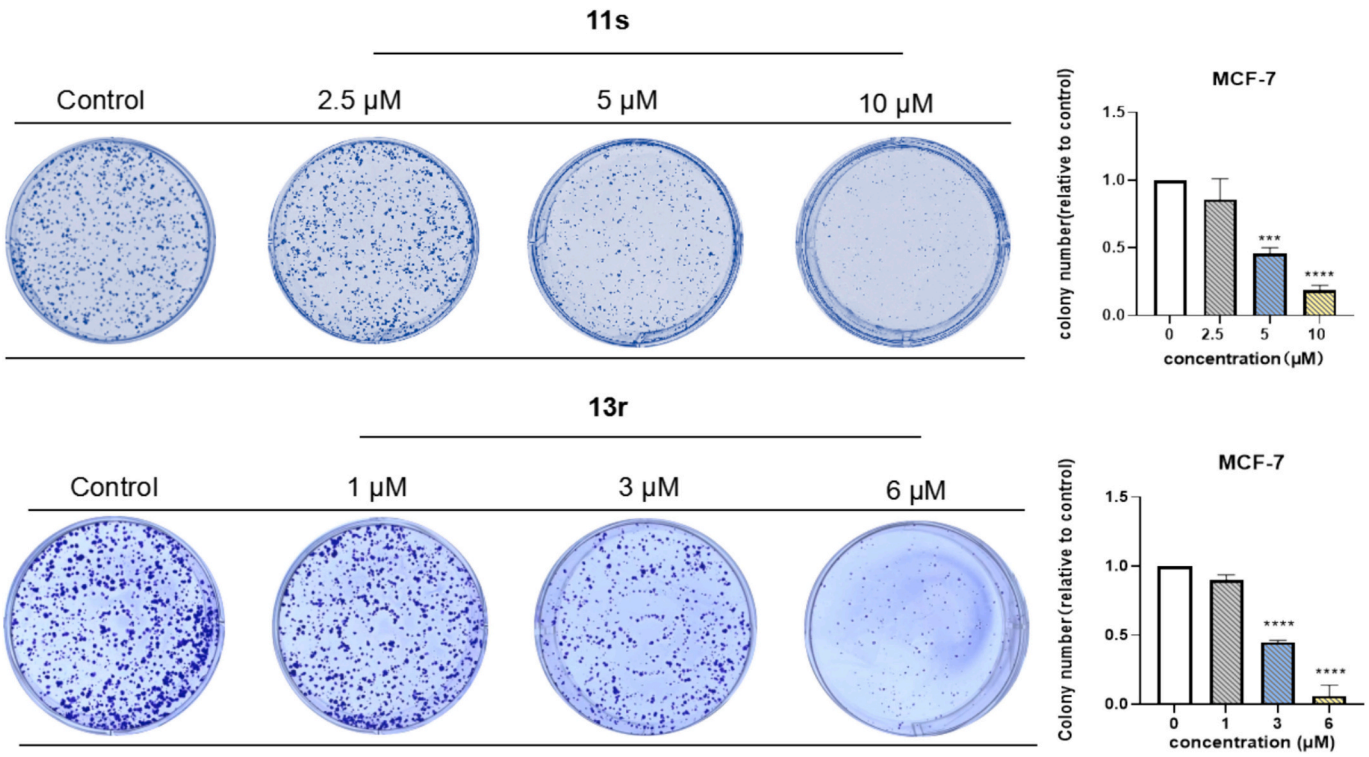

Fig. 6. Colony formation results for non-treated MCF-7 cells and those subjected to 2 weeks of gradient compound **11s** (0, 2.5, 5 and 10 μM) and **13r** (0, 1, 3 and 6 μM) treatment. Data were reported as means ± SDs from a minimum of triplicate independent experiments. $^{**}p < 0.01$, and $^{***}p < 0.001$ vs. solvent control.

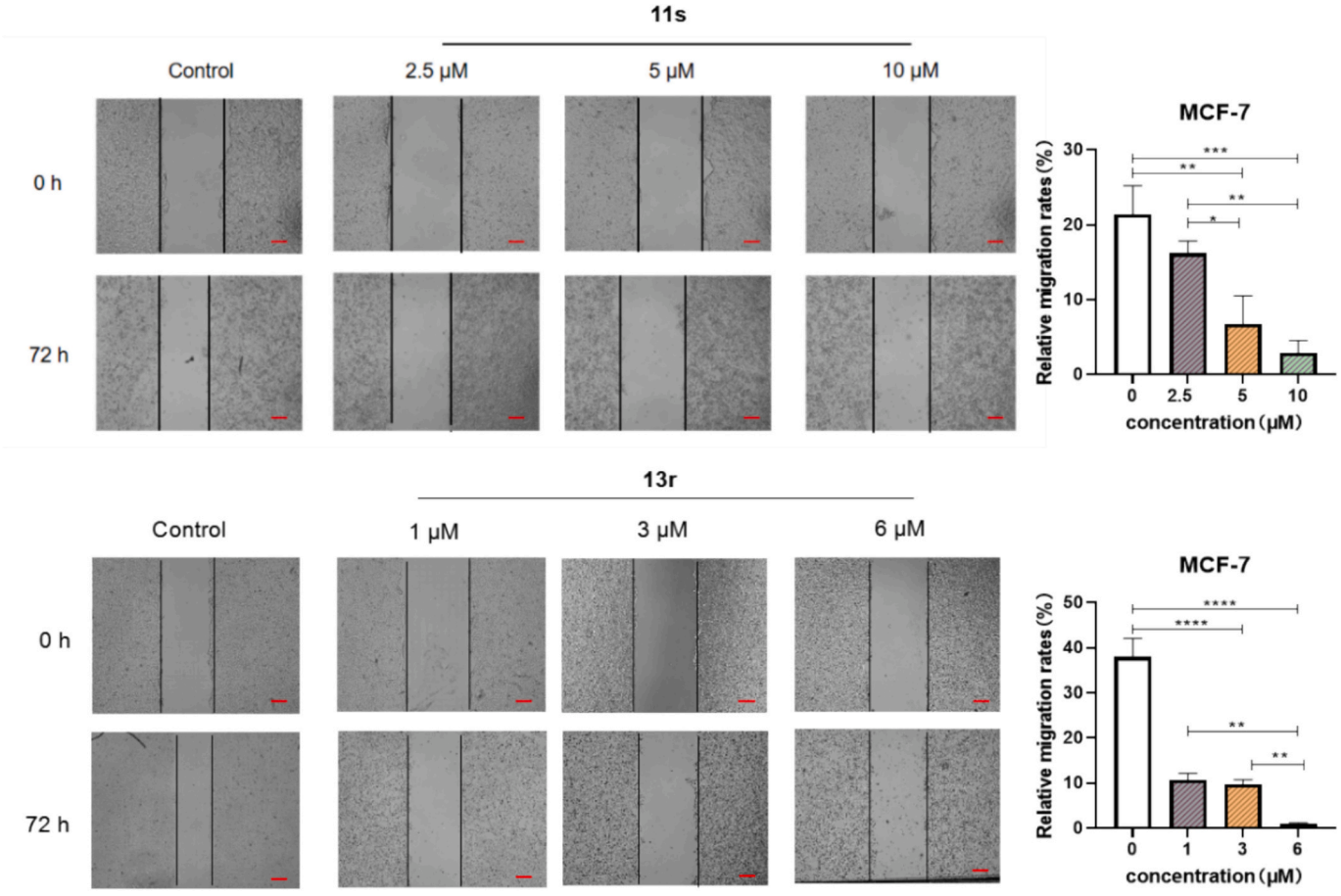

Fig. 7. Effects of **11s** and **13r** on the scratch healing capacity of MCF-7 cells (Scale bar: 250 μm).

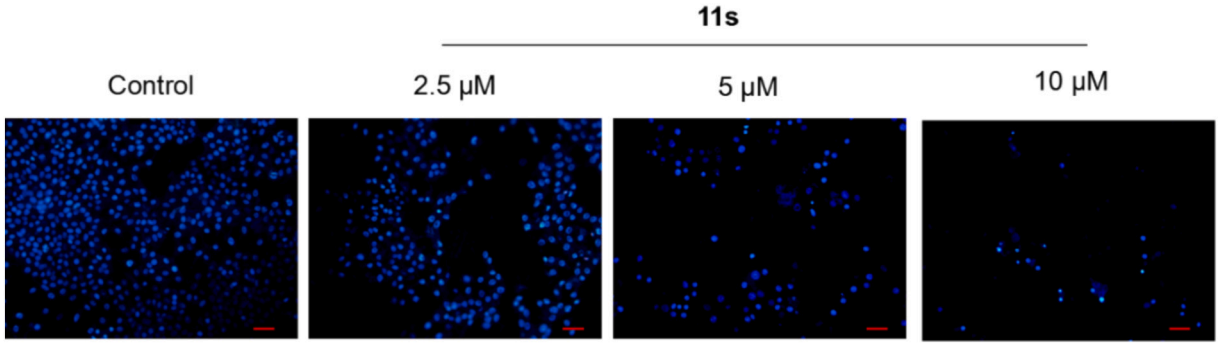

Fig. 8. Compound **11s** caused nuclear changes in MCF-7 cells. Hoechst 33342 assay results for non-treated MCF-7 cells and those subjected to a 24-h gradient compound **11s** (0, 2.5, 5, and 10 μM) treatment. Scale bar, 50 μm.

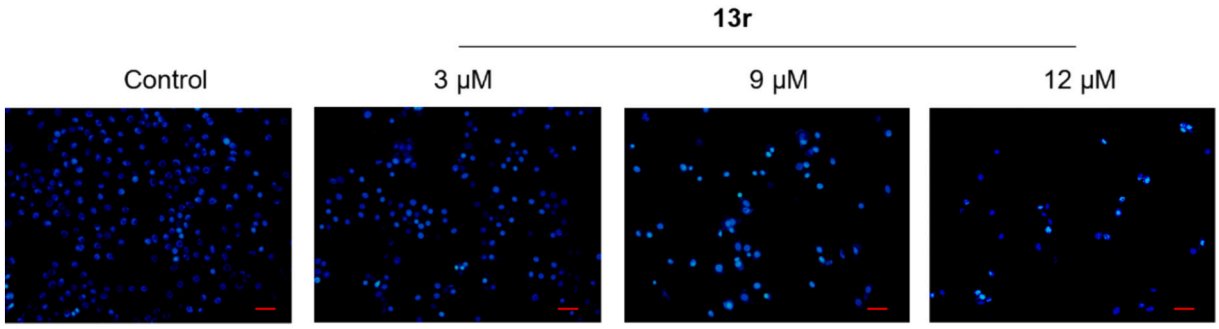

Fig. 9. Compound **13r** caused nuclear changes in MCF-7 cells. Hoechst 33342 assay results for non-treated MCF-7 cells and those subjected to a 24-h gradient compound **13r** (0, 3, 9, 12 μM) treatment. Scale bar, 50 μm.

*2.5. Compounds **11s** and **13r** inhibited the migration of MCF-7 cells*

Breast cancer cells are characterized by high migration and aggressiveness, which are the reasons for poor prognosis in the course of treatment. Cell migration is closely associated with breast cancer metastasis [41,42]. We determined whether the compounds **11s** and **13r** held the ability to inhibit tumor cell migration through the scratch test, since such assay is capable of simulating the process of cancer cell migration *in vivo* to a certain extent. As illustrated in Fig. 7, scratch width in the controls gradually narrowed over time. At 72 h, scratch healing in the dose-dependent group was significantly inhibited with the increase of concentration. Through quantitative analysis, the relative cell mobility with **11s** at a concentration of 10 μM was measured to be 4.36 %, while that with **13r** at a concentration of 6 μM was determined to be 3.37 %, showing significant disparities from the controls (*** $p <$ 0.001). Suggestively, **11s** and **13r** could significantly suppress the MCF-7 cell migration.

*2.6. Compounds **11s** and **13r** elicited apoptosis of MCF-7 cells*

To elucidate the antineoplastic mechanisms of these compounds, we verified whether they could induce apoptosis of MCF-7 cells by Hoechst 33342 staining. Compound treatment resulted in concentration-dependent reductions in cell density, accompanied by apoptotic nuclear morphology, in MCF-7 cells (Figs. 8, 9). Compared with the control group, the compound-treated nucleus gradually crumbled and fragmented, and the bright blue light increased significantly, showing the typical characteristics of nuclear alterations in the apoptotic process. As indicated by these findings, compounds **11s** and **13r** were effective in eliciting the apoptosis of MCF-7 cells. Furthermore, flow cytometry is widely employed in apoptosis research [43]. The fluorochrome-labeling method enables rapid and accurate analysis of large cell populations

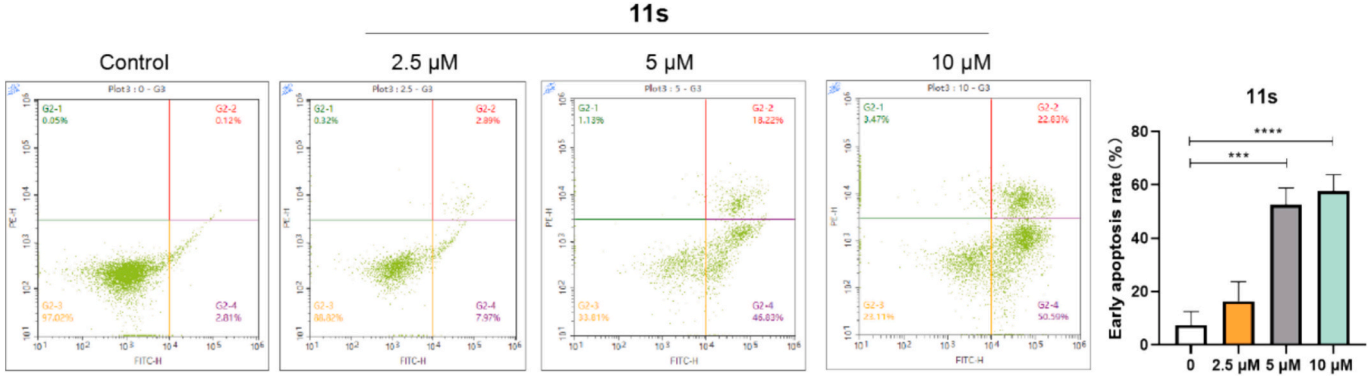

Fig. 10. Flow cytometry results of apoptosis elicited by compound **11s**. Non-treated MCF-7 cells and those subjected to a 24-h **11s** (0, 2.5, 5 and 10 μM) treatment. Combined data from a minimum of triplicate independent experiments are presented. *** $P <$ 0.001 vs. Control.

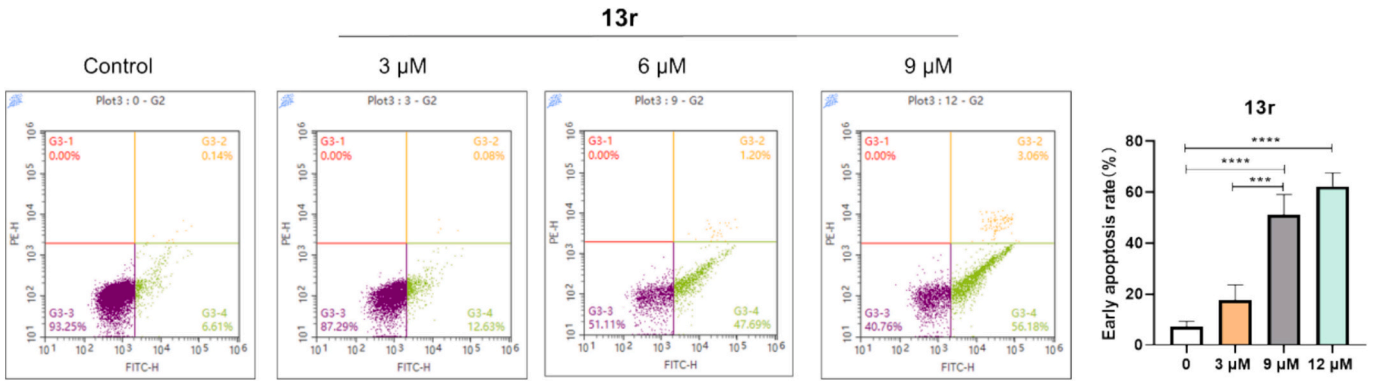

Fig. 11. Flow cytometry results of apoptosis elicited by compound **13r**. Non-treated MCF-7 cells and those subjected to a 24-h **13r** (0, 3, 9, 12 μM) treatment. Combined data from a minimum of triplicate independent experiments are presented. *** $P < 0.001$ vs. Control.

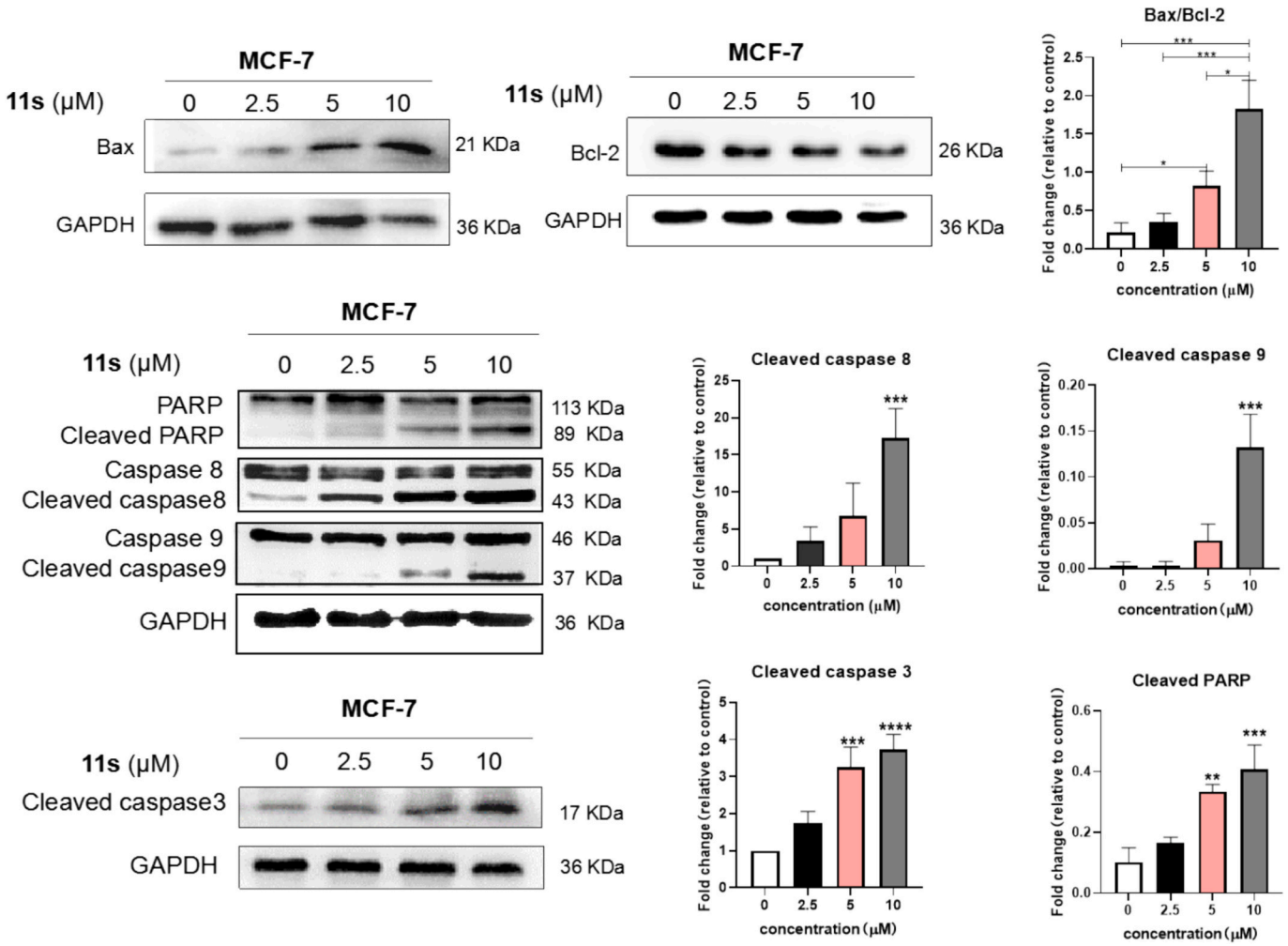

Fig. 12. Western blotting results for alterations in apoptosis-associated proteins following treatment with compound **11s**. Combined data from a minimum of triplicate independent experiments are presented. *$P < 0.05$, and ***$P < 0.001$ vs. Control.

[44]. During apoptosis induction, loss of cell membrane asymmetry results in phosphatidylserine exposure on the outer leaflet of the plasma membrane [45]. Subsequently, we employed flow cytometry to ascertain whether **11s** and **13r** exerted apoptosis-inducing effects. As depicted in Figs. 10 and 11, MCF-7 underwent certain degrees of apoptosis following a 24-h treatment with **11s** and **13r**. In particular, the apoptosis rate of **11s** at 10 μM exceeded 70 %, and that of **13r** at 10 μM differed significantly from the corresponding control value (*** $p < 0.001$). As suggested by the above findings, **11s** and **13r** were capable of inducing MCF-7 cell apoptosis.

2.7. *Impact of compounds **11s** and **13r** on apoptosis-associated proteins*

Cell death modes primarily encompass apoptosis, programmed necrosis, pyroptosis, and iron-dependent death; among these, apoptosis remains the most prevalent mode induced by anticancer drugs [46]. As

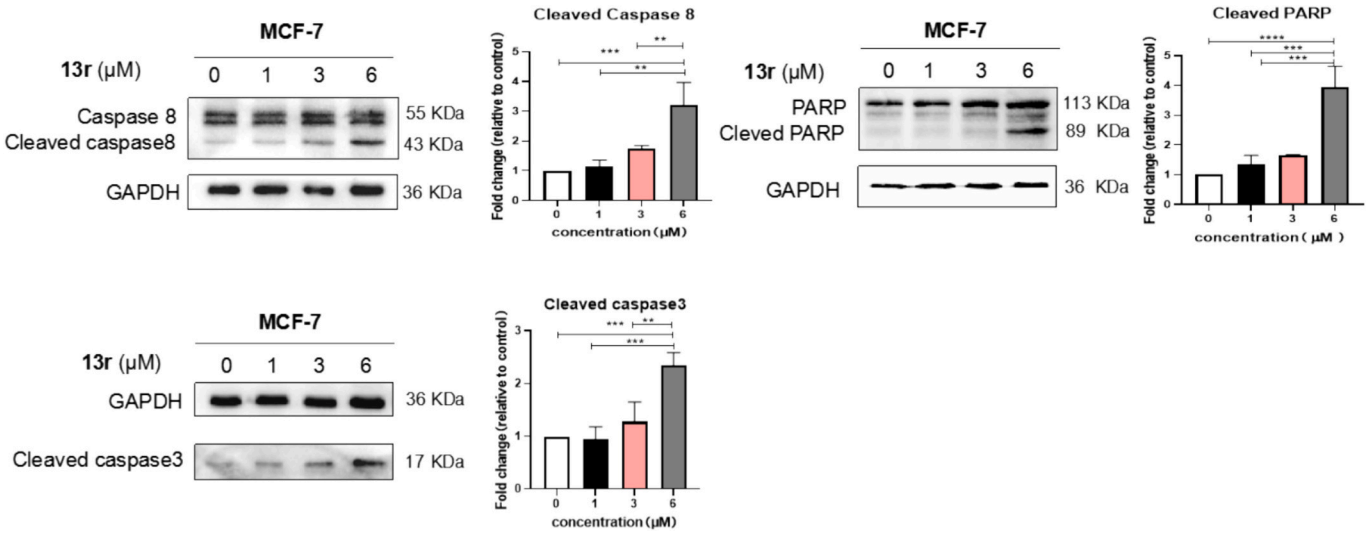

Fig. 13. Western blotting results for alterations in apoptosis-associated proteins following treatment with compound **13r**. Data shown were representative of a minimum of triplicate independent experiments. $^{*}P < 0.05$, and $^{***}P < 0.001$ vs. Control.

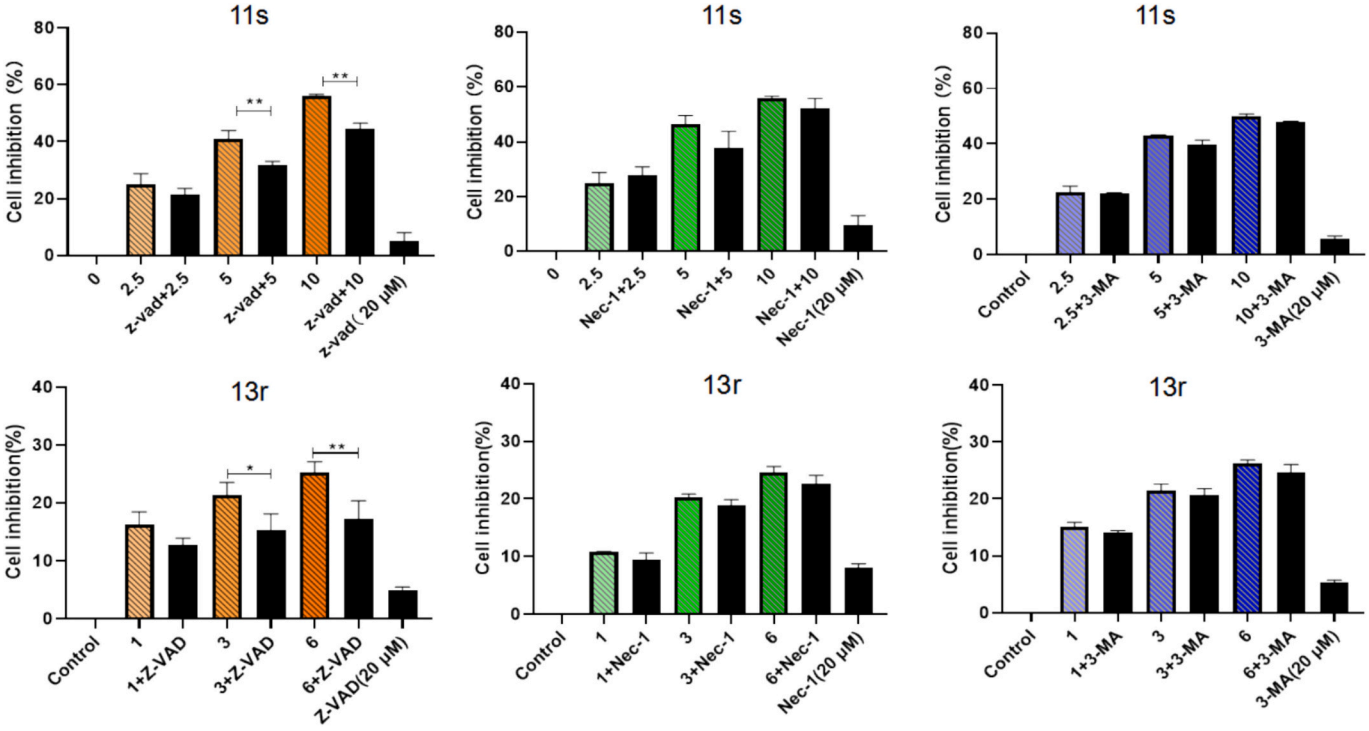

Fig. 14. The changes in cell viability after treatment with compounds **11s** and **13r** using three different inhibitors. Data shown were representative of a minimum of triplicate independent experiments. $^{*}P < 0.05$ and $^{**}p < 0.01$ vs. Control.

the most important death mode of cancer cells, apoptosis can be categorized into exogenous and endogenous types. Exogenous cell apoptosis is generally stimulated by death receptors (e.g., tumor necrosis factor receptor TNFR1/2) after receiving cell death signals, followed by generation of a series of cascades mediated by caspases−8 and −3 [47]. Finally, apoptotic bodies are formed and cleared by macrophages. As for endogenous apoptosis, it is generally induced by DNA damage, mediated by B-cell lymphoma (Bcl) family molecules and downstream caspases−9 and −3 [48,49]. The final clearance mode is similar to that of exogenous apoptosis. To further determine whether compounds **11s** and **13r** induced MCF-7 cell death through apoptotic pathways, variations of apoptosis-related protein levels were examined through Western blotting. Our results demonstrated a significant elevation in Bax/Bcl-2 ratio following the **11s** treatment. In addition, the cracked caspases−3, −9, and −8 alongside cracked PARP levels increased concentration-dependently under **11s** treatment (Fig. 12). These findings suggested that compound **11s** induced MCF-7 cell apoptosis via both the exogenous and endogenous pathways. Furthermore, concentration-dependent elevations in cleaved caspases−3, −8, and PARP levels were noted in the **13r**-treated MCF-7 cells (Fig. 13). These results indicated that compound **13r** promoted apoptosis in MCF-7 cells via an exogenous pathway.

2.8. Effects of inhibitors on compounds *11s* and *13r*

Based on the Western blotting results, it was demonstrated that compounds **11s** and **13r** induce cell apoptosis through the cascade reaction of the caspase pathway. Therefore, we employed the caspase inhibitor *Z*-VAD to investigate its impact on the cytotoxicity of the compounds [50]. As shown in Fig. 14, Z-VAD exhibited no toxicity toward breast cancer cells. However, the addition of Z-VAD significantly reversed the cytotoxic effects of compounds **11s** and **13r**, which was consistent with the Western blotting findings.

To further explore whether compounds **11s** and **13r** induce apoptosis through alternative pathways, we also examined the effects of the autophagy inhibitor 3-MA and the necroptosis inhibitor Nec-1 on the cytotoxicity of the compounds [51,52]. The experimental data revealed that neither 3-MA nor Nec-1 significantly reversed the pro-apoptotic effects of compounds **11s** and **13r**.

In conclusion, our results indicate that compounds **11s** and **13r** induce apoptosis in MCF-7 cells primarily via the caspase-dependent cascade pathway.

3. Conclusion

In the present study, we synthesized a series of phenylamino-benzyl piperazine derivatives through the incorporation of anilines or aliphatic amines, and piperazine moieties. The resulting derivatives were subjected to a comprehensive HRMS, ^{1}H NMR, and ^{13}C NMR characterization procedure. Compound **11s** was found to elicit MCF-7 cell apoptosis via the mitochondrial pathway by activating cleavage of caspase−9, thereby inducing the fragmentation of DNA repair protein PARP. Additionally, both compounds **11s** and **13r** can induce caspase−8 cleavage, subsequently initiating cleavage of caspase−3 and its downstream protein PARP to culminate in the extrinsic apoptosis of MCF-7 cells. We subsequently validated that compounds **11s** and **13r** induce apoptosis in MCF-7 cells through the caspase pathway cascade reaction by using caspase inhibitors. In contrast, neither autophagy nor necrosis inhibitors significantly reversed the cytotoxicity of the compounds, demonstrating that compounds **11s** and **13r** do not induce apoptosis through these two pathways. To sum up, structural modifications on the compounds can trigger cell death via distinct apoptotic pathways. The findings of this study would provide a rational basis for designing potent and low-toxicity anti-breast cancer lead compounds derived from alepterolic acid.

CRediT authorship contribution statement

Xin Wang: Writing – original draft, Investigation. **Lian Ma:** Writing – original draft, Investigation. **Yanchun Sun:** Writing – original draft, Investigation. **Zixuan Tong:** Investigation. **Binbin Zhang:** Investigation. **Yating Jia:** Investigation. **Xiling Dai:** Writing – review & editing, Supervision, Resources, Project administration. **Jianguo Cao:** Writing – review & editing, Supervision, Project administration, Conceptualization. **Guozheng Huang:** Writing – review & editing, Supervision, Conceptualization.

Declaration of competing interest

The authors declare that they have no known competing financial interests or personal relationships that could have appeared to influence the work reported in this paper.

Acknowledgements

This project was supported by Science and Technology Project of Ma'anshan City (No. 2022KN-11), and startup funds from Anhui University of Technology.

Appendix A. Supplementary data

General information for chemical synthesis, protocols for biological evaluation, and the copies of NMR and HRMS spectrum can be found online at https://doi.org/10.1016/j.bioorg.2025.108931.

Data availability

Data will be made available on request.

References

[1] H. Sun, R. Sun, X. Song, W. Gu, Y. Shao, Mechanism and clinical value of exosomes and exosomal contents in regulating solid tumor radiosensitivity, J. Transl. Med. 20 (2022) 189.
[2] H. Sung, J. Ferlay, R.L. Siegel, M. Laversanne, I. Soerjomataram, A. Jemal, F. Bray, Global Cancer Statistics, GLOBOCAN estimates of incidence and mortality worldwide for 36 cancers in 185 countries, CA Cancer J. Clin. 71 (2021) (2020) 209–249.
[3] A.G. Waks, E.P. Winer, Breast Cancer treatment: a review, JAMA 321 (2019) 288–300.
[4] S. Hashem, T.A. Ali, S. Akhtar, S. Nisar, G. Sageena, S. Ali, S. Al-Mannai, L. Therachiyil, R. Mir, I. Elfaki, M.M. Mir, F. Jamal, T. Masoodi, S. Uddin, M. Singh, M. Haris, M. Macha, A.A. Bhat, Targeting cancer signaling pathways by natural products: exploring promising anti-cancer agents, Biomed. Pharmacother. 150 (2022) 113054.
[5] L.I. Ji-Xin, L.I. Yi-Ran, L. Jun, K. Ling-Yi, Highlights of natural products research from China in 2018, Acta Pharm. Sin. (2019) 1333–1347.
[6] O.P.S. Patel, R.M. Beteck, L.J. Legoabe, Exploration of artemisinin derivatives and synthetic peroxides in antimalarial drug discovery research, Eur. J. Med. Chem. 213 (2021) 113193.
[7] H.J. Long, Paclitaxel (Taxol): a novel anticancer chemotherapeutic drug, Mayo Clin. Proc. 69 (1994) 341–345.
[8] A. Ofoegbu, E.B. Ettienne, Pharmacogenomics and morphine, J. Clin. Pharmacol. 61 (2021) 1149–1155.
[9] N. Gregoire, A. Chauzy, J. Buyck, B. Rammaert, W. Couet, S. Marchand, Clinical pharmacokinetics of daptomycin, Clin. Pharmacokinet. 60 (2021) 271–281.
[10] H. Jiang, M. Xiong, Q. Bi, Y. Wang, C. Li, Self-enhanced targeted delivery of a cell wall– and membrane-active antibiotics, daptomycin, against staphylococcal pneumonia, Acta Pharm. Sin. B 6 (2016) 319–328.
[11] M.T. Islam, Diterpenes and their derivatives as potential anticancer agents, Phytother. Res. 31 (2017) 691–712.
[12] V.B. Tatipamula, C.V. Thonangi, T.C. Dakal, G.S. Vedula, B. Dhabhai, H. Polimati, A. Akula, H.T. Nguyen, Potential anti-hepatocellular carcinoma properties and mechanisms of action of clerodane diterpenes isolated from *Polyalthia longifolia* seeds, Sci. Rep. 12 (2022) 9267.
[13] L. Zeng, Q. Wu, T. Wang, L.P. Li, X. Zhao, K. Chen, J. Qian, L. Yuan, H. Xu, W. J. Mei, Selective stabilization of multiple promoter G-quadruplex DNA by using 2-phenyl-1H-imidazole-based tanshinone IIA derivatives and their potential suppressing function in the metastatic breast cancer, Bioorg. Chem. 106 (2021) 104433.
[14] Z. Guan, J. Chen, X. Li, N. Dong, Tanshinone IIA induces ferroptosis in gastric cancer cells through p53-mediated SLC7A11 down-regulation, Biosci. Rep. 40 (2020). BSR20201807.
[15] J. Yu, S. Li, X. Zeng, J. Song, S. Hu, S. Cheng, C. Chen, H. Luo, W. Pan, Design, synthesis, and evaluation of proliferation inhibitory activity of novel L-shaped ortho-quinone analogs as anticancer agents, Bioorg. Chem. 117 (2021) 105383.
[16] Q. Zhao, C. Qing, X.J. Hao, J. Han, G.Y. Zuo, C. Zou, G.L. Xu, Cytotoxicity of labdane-type diterpenoids from *Hedychium forrestii*, Chem Pharm Bull (Tokyo) 56 (2008) 210–212.
[17] Y. Zhao, A. Li, X. Liu, S. Tang, Y. Wang, Q. Zhao, H. Pu, Synthesis and cytotoxicity evaluation of yunnancoronarin a derivatives, Nat. Prod. Res. 1-8 (2025).
[18] Z.Q. Yu, H.X. Du, S. Gao, C.Z. Liang, Eriocalyxin B ameliorated experimental autoimmune prostatitis via modulation of macrophage polarization through gut microbiota-mediated vitamin D(3) alteration, Phytomedicine 135 (2024) 156191.
[19] R. Kaur, A. Bhardwaj, S. Gupta, Cancer treatment therapies: traditional to modern approaches to combat cancers, Mol. Biol. Rep. 50 (2023) 9663–9676.
[20] R.J. Peters, Two rings in them all: the labdane-related diterpenoids, Nat. Prod. Rep. 27 (2010) 1521–1530.
[21] G. Gong, Y.-L. Shen, H.-Y. Lan, J.-M. Jin, P. An, L.-J. Zhang, L.-L. Chen, W. Peng, X. Luan, H. Zhang, The Cyr61 is a potential target for Rotundifuran, a natural labdane-type diterpene from *Vitex trifolia* L., to trigger apoptosis of cervical cancer cells, Oxidative Med. Cell. Longev. 2021 (2021) 6677687.
[22] Q.T.N. Tran, W.S.F. Wong, C.L.L. Chai, Labdane diterpenoids as potential anti-inflammatory agents, Pharmacol. Res. 124 (2017) 43–63.
[23] P. Kapewangolo, J.J. Omolo, R. Bruwer, P. Fonteh, D. Meyer, Antioxidant and anti-inflammatory activity of *Ocimum labiatum* extract and isolated labdane diterpenoid, J. Inflamm. 12 (2015) 4.
[24] R. Acquaviva, G.A. Malfa, M.R. Loizzo, J. Xiao, S. Bianchi, R. Tundis, Advances on natural abietane, labdane and clerodane diterpenes as anti-cancer agents: sources and mechanisms of action, Molecules 27 (2022) 4791.

[25] T. Soumya, T. Lakshmipriya, K.D. Klika, P.R. Jayasree, P.R. Manish Kumar, Anticancer potential of rhizome extract and a labdane diterpenoid from *Curcuma mutabilis* plant endemic to Western Ghats of India, Sci. Rep. 11 (2021) 552.
[26] Y.-Y. Chen, X.-T. Zeng, D.-Q. Xu, S.-J. Yue, R.-J. Fu, X. Yang, Z.-X. Liu, Y.-P., Tang, Pimarane, abietane, and labdane diterpenoids from *Euphorbia pekinensis* Rupr. and their anti-tumor activities, Phytochemistry 197 (2022) 113113.
[27] S. Zhang, N. Feng, J. Huang, M. Wang, L. Zhang, J. Yu, X. Dai, J. Cao, G. Huang, Incorporation of amino moiety to alepterolic acid improve activity against cancer cell lines: synthesis and biological evaluation, Bioorg. Chem. 98 (2020) 103756.
[28] N. Wang, L. Zhang, J. Yu, K. Chang, M. Fan, Z. Liu, L. Ma, J. Cao, G. Huang, Identification of an alepterolic acid derivative as a potent anti-breast-cancer agent via inhibition of the Akt/p70^{S6K} signaling pathway, Chem. Biodivers. 21 (2024) e202301248.
[29] X. Wang, L. Qin, L. Ma, X. Dai, G. Huang, J. Cao, Benzylpiperazinyl derivatives of alepterolic acid: synthesis and cytotoxic evaluation, Chem. Biodivers. 22 (2025) e202401706.
[30] M. Al-Ghorbani, M.A. Gouda, M. Baashen, O. Alharbi, F.A. Almalki, L. V. Ranganatha, Piperazine heterocycles as potential anticancer agents: a review, Pharm. Chem. J. 56 (2022) 29–37.
[31] A.K. Rathi, R. Syed, H.-S. Shin, R.V. Patel, Piperazine derivatives for therapeutic use: a patent review (2010-present), Expert Opin. Ther. Pat. 26 (2016) 777–797.
[32] R.-H. Zhang, H.-Y. Guo, H. Deng, J. Li, Z.-S. Quan, Piperazine skeleton in the structural modification of natural products: a review, J. Enzyme Inhib. Med. Chem. 36 (2021) 1165–1197.
[33] M. Shaquiquzzaman, G. Verma, A. Marella, M. Akhter, W. Akhtar, M.F. Khan, S. Tasneem, M.M. Alam, Piperazine scaffold: a remarkable tool in generation of diverse pharmacological agents, Eur. J. Med. Chem. 102 (2015) 487–529.
[34] T.J. Schumacher, N. Sah, K. Palle, J. Rumbley, V.R. Mereddy, Synthesis and biological evaluation of benzofuran piperazine derivatives as potential anticancer agents, Bioorg. Med. Chem. Lett. 93 (2023) 129425.
[35] R. Morigi, A. Locatelli, A. Leoni, M. Rambaldi, Recent patents on thiazole derivatives endowed with antitumor activity, Recent Pat. Anticancer Drug Discov. 10 (2015) 280–297.
[36] X. Wang, Y. Zhuang, Y. Wang, M. Jiang, L. Yao, The recent developments of camptothecin and its derivatives as potential anti-tumor agents, Eur. J. Med. Chem. 260 (2023) 115710.
[37] G. Fan, X. Luo, Y. Shi, Y. Wang, L. Ji, Y. Gong, E. Yang, C. Chen, S. Cui, H. Ding, Z. Zhang, J. Wang, Y. Liu, Z. Wang, FL118: a potential bladder cancer therapeutic compound targeting H2A.X identified through library screening, Bioorg. Chem. 153 (2024) 107802.
[38] M. Bou Saleh, A. Louvet, L.C. Ntandja-Wandji, E. Boleslawski, V. Gnemmi, G. Lassailly, S. Truant, F. Maggiotto, M. Ningarhari, F. Artru, E. Anglo, P. Sancho-Bru, A. Corlu, J. Argemi, J. Dubois-Chevalier, S. Dharancy, J. Eeckhoute, R. Bataller, P. Mathurin, L. Dubuquoy, Loss of hepatocyte identity following aberrant YAP activation: a key mechanism in alcoholic hepatitis, J. Hepatol. 75 (2021) 912–923.
[39] D. Park, E. Wershof, S. Boeing, A. Labernadie, R.P. Jenkins, S. George, X. Trepat, P. A. Bates, E. Sahai, Extracellular matrix anisotropy is determined by TFAP2C-dependent regulation of cell collisions, Nat. Mater. 19 (2020) 227–238.
[40] B. Wang, R. Shi, W. Du, J. Guo, N. He, Y. Zhu, H. Yu, H. Lu, L. Zhong, X. Li, W. Zhou, F. Yang, X. Feng, Prodigiosin inhibits proliferation and induces apoptosis through influencing amino acid metabolism in multiple myeloma, Bioorg. Chem. 159 (2025) 108349.
[41] T. Kanoh, J. Lu, T. Mizoguchi, M. Itoh, The E3 ubiquitin ligase MIB1 suppresses breast cancer cell migration through regulating CTNND1 protein level, Biochem. Biophys. Res. Commun. 667 (2023) 73–80.
[42] M. Kamo, M. Ito, T. Toma, H. Gotoh, R. Shimozono, R. Nakagawa, R. Koga, K. Monde, H. Tateishi, S. Misumi, M. Otsuka, M. Fujita, Discovery of anti-cell migration activity of an anti-HIV heterocyclic compound by identification of its binding protein hnRNPM, Bioorg. Chem. 107 (2021) 104627.
[43] J.M. Roldán-Peña, A. Puerta, J. Dinić, S. Jovanović Stojanov, A. González-Bakker, F.J. Hicke, A. Mishra, A. Piyasaengthong, I. Maya, J.W. Walton, M. Pešić, J. M. Padrón, J.G. Fernández-Bolaños, Ó. López, Biotinylated selenocyanates: potent and selective cytostatic agents, Bioorg. Chem. 133 (2023) 106410.
[44] M. Eray, M. Mättö, M. Kaartinen, L. Andersson, J. Pelkonen, Flow cytometric analysis of apoptotic subpopulations with a combination of annexin V-FITC, propidium iodide, and SYTO 17, Cytometry 43 (2001) 134–142.
[45] G. Koopman, C.P. Reutelingsperger, G.A. Kuijten, R.M. Keehnen, S.T. Pals, M. H. van Oers, Annexin V for flow cytometric detection of phosphatidylserine expression on B cells undergoing apoptosis, Blood 84 (1994) 1415–1420.
[46] K. Newton, A. Strasser, N. Kayagaki, V.M. Dixit, Cell death, Cell 187 (2024) 235–256.
[47] J. Medler, H. Wajant, Tumor necrosis factor receptor-2 (TNFR2): an overview of an emerging drug target, Expert Opin. Ther. Targets 23 (2019) 295–307.
[48] D.L. Vaux, S. Cory, J.M. Adams, Bcl-2 gene promotes haemopoietic cell survival and cooperates with c-myc to immortalize pre-B cells, Nature 335 (1988) 440–442.
[49] A.A. Muravev, A.D. Voloshina, A.S. Sapunova, F.B. Gabdrakhmanova, O.A. Lenina, K.A. Petrov, S. Shityakov, E.V. Skorb, S.E. Solovieva, I.S. Antipin, Calix[4]arene-pyrazole conjugates as potential cancer therapeutics, Bioorg. Chem. 139 (2023) 106742.
[50] M.E. Pero, G. Zullo, L. Esposito, A. Iannuzzi, P. Lombardi, C. De Canditiis, G. Neglia, B. Gasparrini, Inhibition of apoptosis by caspase inhibitor Z-VAD-FMK improves cryotolerance of in vitro derived bovine embryos, Theriogenology 108 (2018) 127–135.
[51] Y. Dong, Y. Wu, G.L. Zhao, Z.Y. Ye, C.G. Xing, X.D. Yang, Inhibition of autophagy by 3-MA promotes hypoxia-induced apoptosis in human colorectal cancer cells, Eur. Rev. Med. Pharmacol. Sci. 23 (2019) 1047–1054.
[52] K.Y. Shao, S.D. Luo, E.Y. Huang, T.M. Chang, L. Botcha, M. Sehar, J.F. Liu, P. K. Chuang, Acetylshikonin induces cell necroptosis via mediating mitochondrial function and oxidative stress-regulated signaling in human oral cancer cells, Bioorg. Chem. 159 (2025) 108396.